



Received on 15 December 2020; received in revised form, 11 March 2021; accepted, 26 May 2021; published 01 November 2021

PHARMACOPHORE BASED MODELLING OF PYRIDINE-PYRIMIDINE ANALOGS AS MER TYROSINE KINASES INHIBITORS IN ANTICANCER THERAPY

Sandip Wagh* and Vaibhav Wagh

Department of Pharmaceutical Chemistry, SNJB's SSDJ College of Pharmacy, Neminagar, Chandwad, Nasik - 423101, Maharashtra, India.

Keywords:

MERTK inhibitors, Molecular Docking, Pharmacophore, Pyridine-Pyrimidine, PHASE

Correspondence to Author:

Mr. Sandip Wagh

Assistant Professor,
Department of Pharmaceutical
Chemistry, SNJB's SSDJ College of
Pharmacy, Neminagar, Chandwad,
Nasik - 423101, Maharashtra, India.

E-mail: sandipwagh2911@gmail.com

ABSTRACT: MER kinase is an important tyrosine-kinase receptor that is associated with a variety of cancers, including mantle cell lymphomas, pituitary adenomas and T-cell acute lymphoblastic leukemia. Identification of new MERTK inhibitors assumes crucial importance. Only one ligand-based pharmacophore model is reported to date for MERTK inhibitors. There are many more molecules with improved enzyme inhibitory activity reported since the publishing of this model. Because of this fact, we decided to develop a pharmacophore model for the MERTK inhibitors to assist in virtual screening using Phase for this purpose. Hydrogen bond donors, hydrogen bond acceptors, rings, positively ionizable groups, and hydrophobic groups were considered as key elements contributing to ligand activity for the pharmacophore model. Pharmacophore modelling was followed by extensive validation of the developed pharmacophore models. The developed pharmacophore model highlighted the importance of the positively ionizable groups and a ring structure. We have used these models for database screening to arrive at few hits. So findings in this study were proved to be useful in the optimization and discovery of MERTK inhibitors with a new scaffold.

INTRODUCTION: MERTK is a member of the TAM (TYRO3, AXL, and MERTK) family of receptor tyrosine kinases (RTK) which share growth arrest specific-6 (gas6) is a common biological ligand^{1, 27, 28, 29}. Other ligands, including Protein S, Tubby, TULP-1, and Galectin-3 can also stimulate Mer. Under normal physiological conditions, Mer mediates the second phase of platelet aggregation, macrophage, and epithelial cell clearance of apoptotic cells^{2, 3, 4}.

It also modulates macrophage cytokine synthesis, cell motility and cell survival⁵. Abnormal activation or overexpression of Mer RTK has been implicated in the neoplastic progression of many cancers such as mantle cell lymphoma, pituitary adenoma and T-cell acute lymphoblastic leukemia and has been correlated with poorer prognosis.

Mer is ectopically expressed in most common pediatric malignancies such as B-cell and T-cell acute lymphoblastic leukemia, but it is not expressed in normal mouse and human T- and B-lymphocytes at any stage of development⁶. Inhibition of Mer by si / sh-RNA knockdown sensitizes cells to chemotherapy-induced apoptosis and doubles survival in a xenograft model of acute leukemia. Similar effects are observed when Mer expression is abrogated with shRNA in small-cell

QUICK RESPONSE CODE 	DOI: 10.13040/IJPSR.0975-8232.12(11).5905-15
This article can be accessed online on www.ijpsr.com	
DOI link: http://dx.doi.org/10.13040/IJPSR.0975-8232.12(11).5905-15	

lung cancer (NSCLC) cells⁷. Besides this, the treatment of melanoma cells with a Mer Inhibitor UNC1062 exhibited effects comparable to shRNA-mediated Mer Inhibition, including reduced colony formation in soft agar and decreased invasion into the collagen matrix^{8,9}. This data indicates that Mer is a novel therapeutic target for the treatment of all and other cancers that overexpress Mer. MER-like RTKs consist of extracellular domains that are composed of two tandem N-terminal immunoglobulin-like domains (Igs) followed by two tandem membrane-proximal fibronectin type III-like (FNIII) domains. The intracellular regions of TAMs contain a tyrosine kinases domain that is highly conserved^{10, 11}. MerTK is a single-pass transmembrane protein that transducer extracellular signals to intracellular phosphor signaling pathways influencing cell survival, migration, differentiation, and phagocytic activity.

Mer can drive prometastatic signaling in tumor cells and is over-expressed in a variety of cancer types, including melanoma and colorectal cancer, lung cancer, breast cancer, ovarian cancer, pancreatic cancer, and hepatocarcinoma. Mer signaling can also influence tumor-associated leukocytes, including macrophages to down-regulate their anti-tumor inflammatory responses, poor prognosis and metastasis. Thus, inhibition or genetic silencing of Mer in both cancer cells and leukocytes is effectively limited tumor growth and metastasis. Mer plays a physiological role in efferocytosis, which is the clearing of dying cell debris by phagocytic immune cells. MERTK genetic mutations are associated with the accumulation of such debris, especially in the retina, thus contributing to the degenerative eye disease retinitis pigmentosa. Mer activity in phagocytes mediates processes in infection and sterile inflammation, for instance, during atherosclerosis. Heterogeneity of Mer expression across patients, its role in metastasis throughout the body, its presence across a variety of cell types including both tumor cells and immune cells, and its therapeutic transgenic expression in ophthalmic disease motivate developing methods to non-invasively image at the cellular or subcellular resolution^{12, 13}. Computer-aided drug design (CADD) is a very useful tool in rational drug design to minimize the time for identification, characterization and structure-optimization for

novel drug candidates. CADD methods can be applied to both ligand-based as well as structure-based drug designs. Ligand-based drug design is an indirect approach to facilitate the development of pharmacologically active compounds by studying molecules interacting with the biological target of interest. Step one of any drug design process is the identification of suitable target biomolecules associated with a disease. Usually, a key protein of a biochemical pathway associated with the disease state serves as a potential drug target. After carrying out LBDD, promising molecules are identified being referred to as lead compounds which were then designed to inhibit or promote the concerned biochemical pathway. The next step in the drug discovery process is to optimize the lead molecules to maximize the interactions with the target biomolecule.

LBDD plays a crucial role in guiding the lead optimization process, where these methods are useful in the absence of an experimental 3D structure of the target enzyme. Due to the lack of an experimental structure, the known ligand molecules that bind to the cellular target are studied to understand the structural and physicochemical properties of the ligands that correlate with the desired pharmacological activity. Besides of the known ligand molecules, ligand-based methods may also include natural products or substrate analogs that interact with the target molecule yielding the desired pharmacological effects. This approach takes advantage of the availability of the target 3D structure to identify the nature of the target-ligand interaction and the structural requirements of the ligand to optimize the interaction²³. A ligand-based pharmacophore attempts to identify the essential chemical features of the ligand is required to identify the interactions with the biological macromolecules. However, these pharmacophoric representations are greatly simplified and therefore can't explain the complete biophysical nature of drug interactions. Virtual screening performed using ligand-based pharmacophores results in many false positives because it does not take into account the intricate details about the receptor, such as the shape of the binding and interaction site²⁵. Ligand Based Pharmacophore generation conventionally begins with the ligand preparation and conformation generation²⁴.

Several studies have revealed that the energy of the biological conformer of a particular compound is usually well above its local energy minimum. The induced-fit theory also explains that molecules should rearrange themselves to fit into the active site of the protein and energy spent on rearrangement is compensated by protein-ligand binding. Therefore, no protocol including energy minimization could assure the prediction of the biological confirmation of small molecules. This further limits the applicability of ligand-based pharmacophores²⁵. With the large number of VS approaches available, the users need to learn which one is the optimal method for the target of interest. Thus, the objective assessment for all viable approaches becomes indispensable²⁶. Because of these facts, we have decided to compare the robustness of the ligand-based pharmacophore model methods to select the most appropriate method for virtual screening.

The present work aimed to develop pharmacophore models for pyridine-pyrimidine analogs which act as inhibitors of Mer kinase. Merkinase plays an important role by regulating macrophage activity, platelet aggregation, enhances sensitivity, cellular growth, and cell proliferation. The aim is to develop the best pharmacophore model based on the QSAR equation. This model can be used to design and develop new inhibitors of Merkinase in search of effective anticancer therapy. The dataset used for Ligand Based Pharmacophore generation were as follows:

RESULTS AND DISCUSSION:

Ligand Based Pharmacophore Model: Ligand Based Pharmacophore were generated using Phase (version 20.0.3, Schrodinger, LLC, New York, NY, 2020) implemented in Maestro 12.5.

Generation of Ligand Based Pharmacophore Model using the Selected Datasets: Above Mentioned groups were used for the generation of ligand-based pharmacophore models. Common pharmacophore hypotheses were generated from a set of three to four active ligands in the Pharm Set because they contain important structural features crucial for binding at the receptor-binding site^{15, 21, 22}. It is desirable to include between three to seven points for pharmacophore generation¹⁵. More than seven points in a pharmacophore will not be desirable because all chemical scaffolds may not be able to align exactly during screening and these can be probable inhibitors that may get missed¹⁵. In the find pharmacophore step, we used five minimum sites and five maximum sites to generates an optimum combination of features common to the most active compounds. Five-point pharmacophore hypotheses were generated and subjected to stringent scoring function analysis.

Hypotheses Scoring: Among the various pharmacophores generated, the hypothesis showing the best alignments with the active compounds were identified by aligning the hypothesis with active compounds and calculating the survival score. The survival score function helps in identifying the best hypothesis and ranking all the hypotheses. The selected hypothesis should distinguish between the active and inactive molecules.

Further, to confirm that the pharmacophore hypotheses map well with more active than inactive features, they were aligned to inactive compounds and scored. If inactive ligands score well, the hypothesis may be considered to be poor and should be rejected since it does not distinguish between active and inactive ligands¹⁵.

TABLE 1: SCORE FOR DEVELOPED PHARMACOPHORE HYPOTHESIS

Title	Survival Score	Site Score	Selectivity Score	Inactive Score	Adjusted Score	Phase Hypo score
DDHRR_1	5.253	0.978	1.991	2.251	3.002	1.315
DHHRR_1	5.288	0.884	2.055	2.177	3.05	1.314
DDHRR_2	5.216	0.938	1.995	2.093	3.122	1.313
DDHRR_3	5.207	0.871	2.001	1.816	3.391	1.312
DHHRR_2	5.163	0.818	2.061	2.133	3.03	1.31
DHHRR_3	5.152	0.806	2.046	2.055	3.097	1.309
DHHRR_4	5.144	0.826	2.042	2.01	3.134	1.309
DDHRR_4	5.14	0.855	1.983	2.116	3.025	1.308
DDHRR_5	5.136	0.864	2.001	2.059	3.078	1.308
DDHRR_6	5.136	0.867	2.001	1.937	3.198	1.308

Building QSAR Model: The main purpose of developing the QSAR model was to predict the biological activities of new compounds whereby the generated model would be statistically robust, both internally and externally. The dataset was divided into a training set and a test set. 70% of molecules were taken in the training set and 30% in

the test set. The co-crystallized ligand was included in the training set. Atom-based 3D-QSAR models were generated for hypotheses. The QSAR parameters were used as the second filter for the selection of hypotheses. Only those hypotheses were taken for further studies that had $Q^2 > 0.7$ and Pearson $R > 0.8$.

TABLE 2: SUMMARY OF PHASE 3D-QSAR STATISTICAL RESULTS FOR PHARMACOPHORE MODEL

Hypothesis	SD	R^2	R^{CV}	Stability	F	P	RMSE	Q^2	Pearson R
DHRR-1	0.1070	0.9949	0.6772	0.624	1011.7	6.56e-29	0.61	0.6969	0.9067
DDHRR-1	0.1178	0.9934	0.6218	0.636	786.6	1.69e-27	0.57	0.7827	0.9192

Table 3 shows the equation obtained for pyridine-pyrimidines. **Fig. 1-2** indicates the graphs of observed v/s predicted biological activity based on the 3D-QSAR Statistical results.

Scatter Plot for Best Hypothesis DDHRR_1 for Predicted vs. Experimentally Observed Activities:

The plot of experimental activity v/s phase predicted activity for DDHRR-1 is shown in **Fig 4.9** and **4.10**, respectively. After comparing two hypotheses, DDHRR-1 was selected as the best hypothesis. It has a high value of the coefficient of determination ($R^2=0.9934$) and variance ratio ($F=786.6$), low value of the standard deviation of the regression ($SD=0.1178$), suggesting that it was a statistically significant regression with a great

degree of confidence. The prediction of the training set was a perfect one. Similarly, the test set revealed expected better parameters, the high value of cross-validated value ($Q^2=0.7827$) and Pearson correlation coefficient (Pearson- $R=0.9192$), low value of root mean squared error ($RMSE=0.57$), demonstrating that the prediction of the test set was credible.

These plots exhibit the linear relationship between predicted and actual activity. Thus it can be said that the model developed is highly successful in the prediction of activity test compounds with the least variation as indicated by a standard deviation of 0.1178.

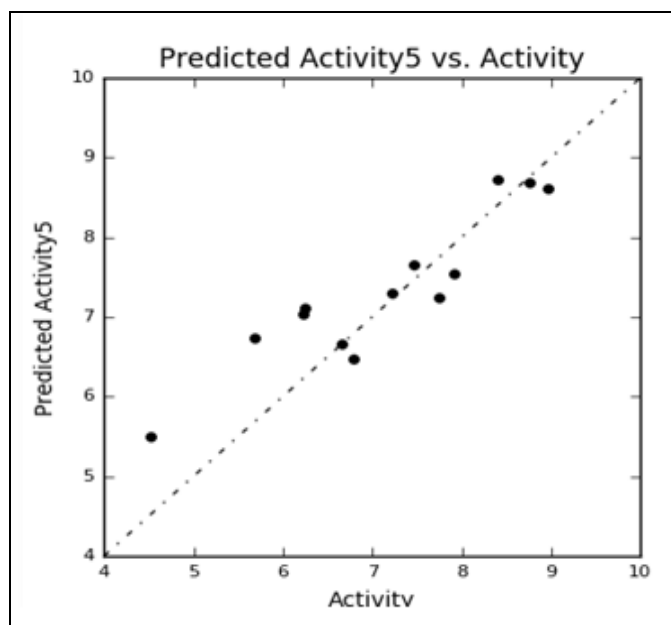


FIG. 1: TEST SET HYPOTHESIS DDHRR_1

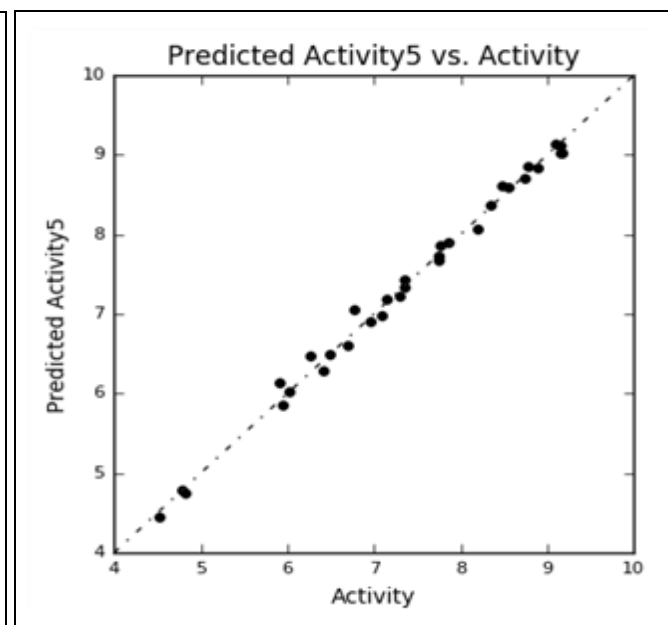


FIG. 2: TRAINING SET HYPOTHESIS DDHRR_1

Superposition of the Most Active, Inactive, all Active, Inactive Compound on the Pharmacophore DDHRR_1: The superposition of the most active compound, least active compound,

most fit compound, and all active compounds on the best pharmacophore hypothesis DDHRR-1 has been given in **Fig. 3-6**.

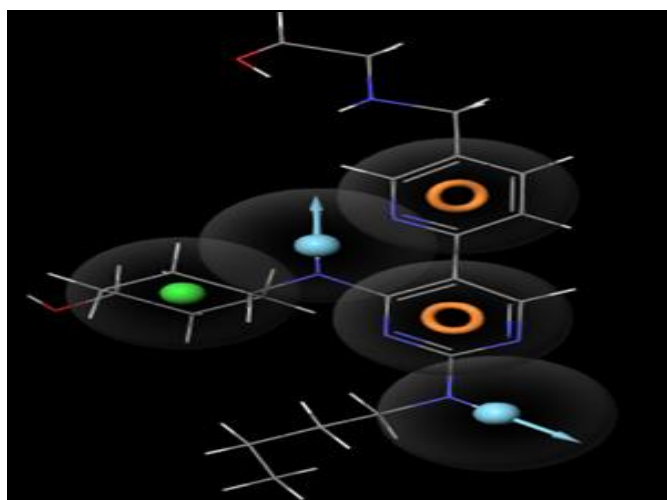


FIG. 3: SUPERPOSITION OF THE MOST ACTIVE COMPOUND ON THE PHARMACOPHORE DDHRR_1

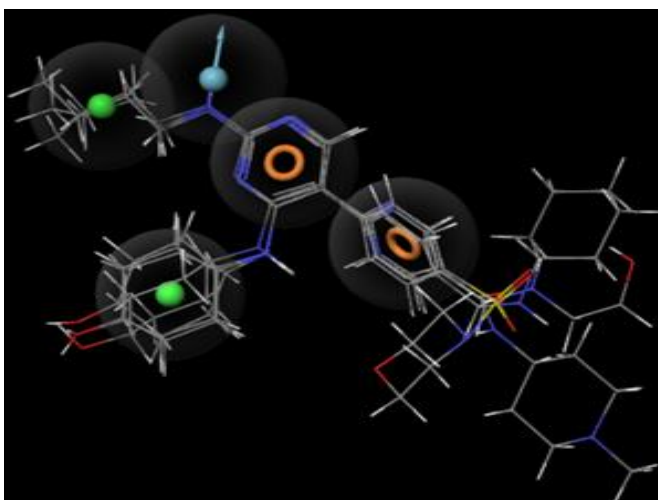


FIG. 4: SUPERPOSITION OF THE MOST INACTIVE COMPOUND ON THE PHARMACOPHORE DDHRR_1

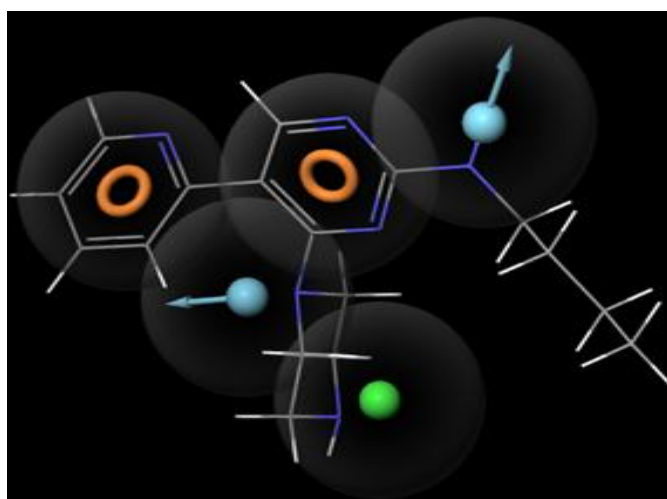


FIG. 5: SUPERPOSITION OF ALL ACTIVES OF THE DATASET ON THE PHARMACOPHORE HYPOTHESIS DDHRR_1

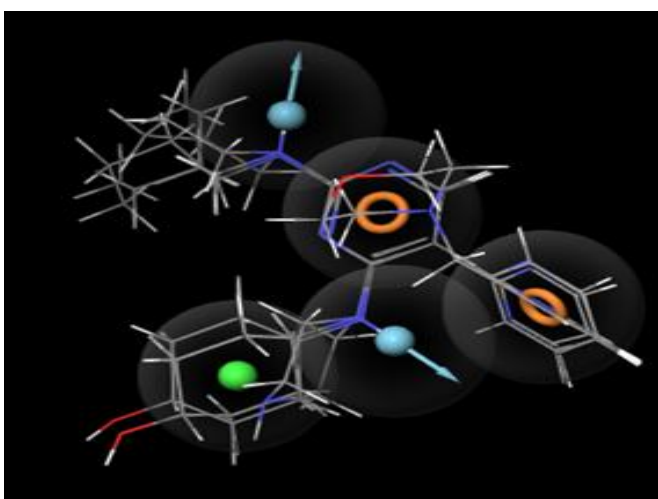


FIG. 6: SUPERPOSITION OF ALL INACTIVES OF THE DATASET ON THE PHARMACOPHORE HYPOTHESIS DDHRR_1

MATERIALS AND METHODS:

Generation of Ligand Based Pharmacophore Selection of Dataset:

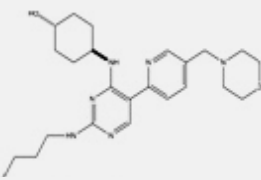
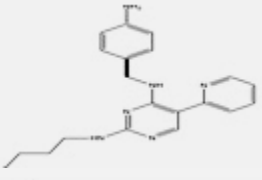
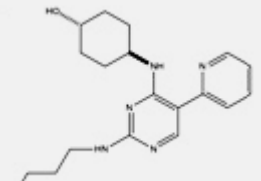
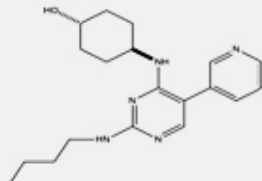
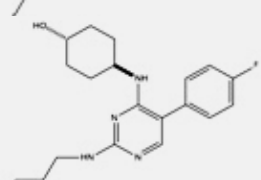
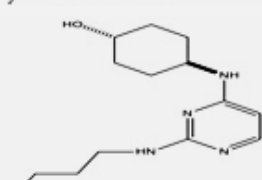
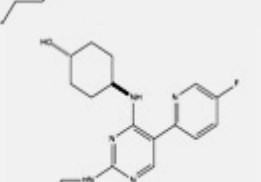
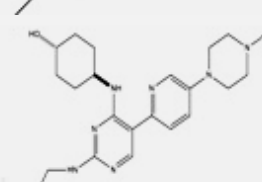
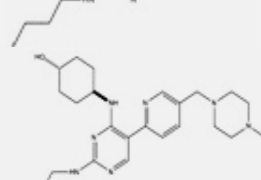
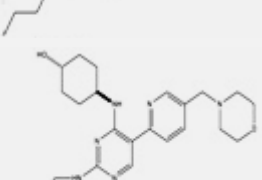
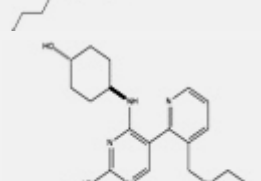
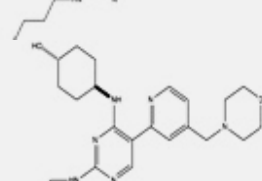
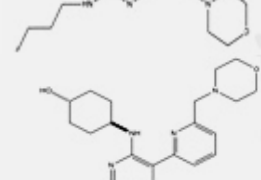
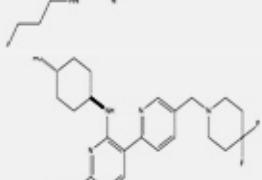
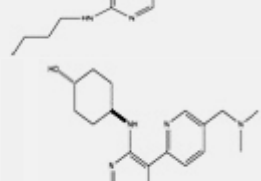
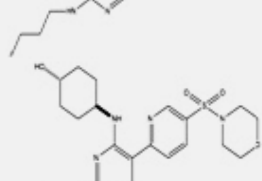
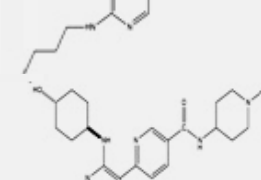
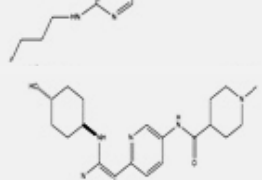
(A) Combined Dataset Generation and 2D-Similarity Analysis: Initially, a dataset consisting of molecules belonging to different chemical classes was used for the generation of ligand-based pharmacophore. However, this approach proved to be unsuccessful. The pharmacophore hypotheses generated by this approach were biased towards the chemical class that was used in its generation and failed to accurately align the molecules from other classes. These hypotheses were found to be statistically poor too. Thus, 2D-Similarity analysis of these molecules was performed using canvas, and Tanimoto coefficients for representative molecules from each class concerning the others were generated. Thus, only those classes whose representative ligands had a Tanimoto coefficient

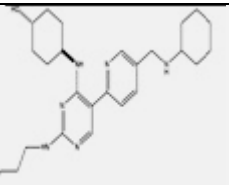
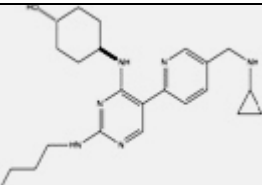
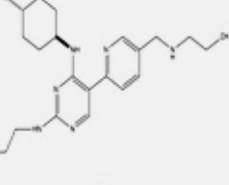
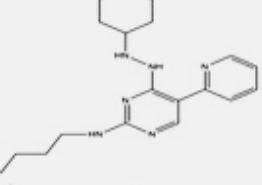
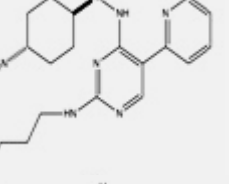
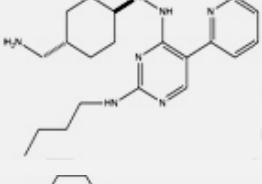
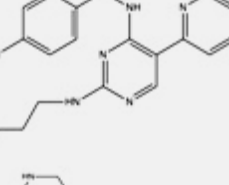
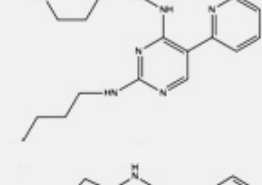
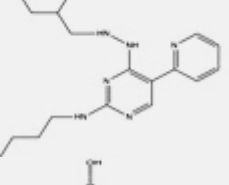
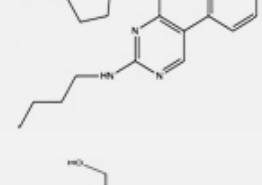
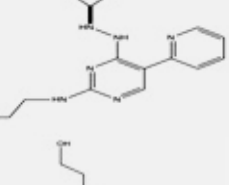
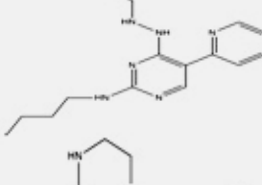
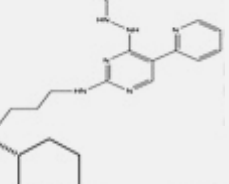
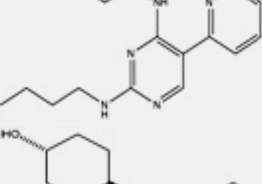
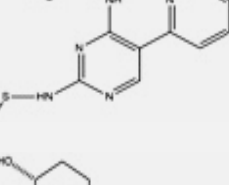
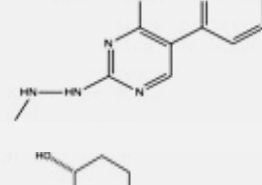
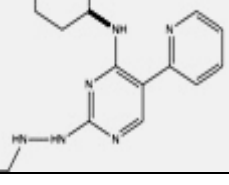
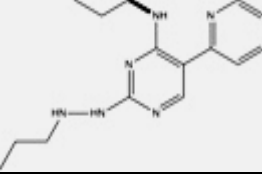
of 0.4 and above were used for combining into a group.

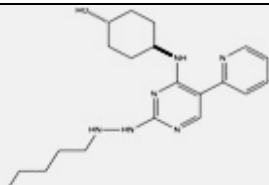
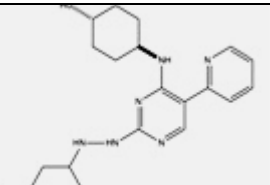
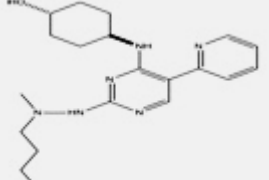
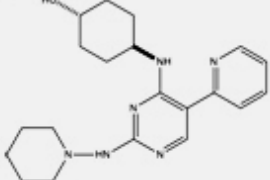
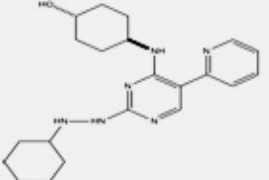
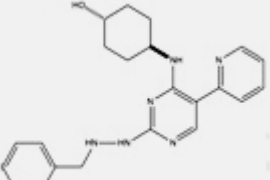
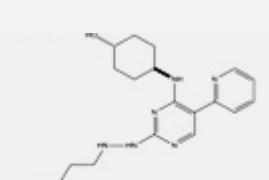
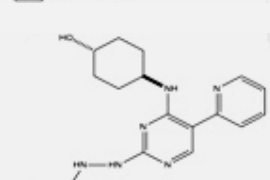
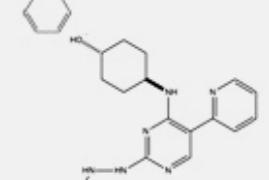
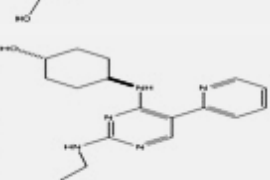
(B) Dataset used: Dataset is used for the present study belonging to the chemical class of pyridine-pyrimidine. Biological activities of sets of compounds were expressed in terms of pIC_{50} whereas the biological activities were expressed in terms of pKi , where, IC_{50} is the concentration of the inhibitor producing 50% inhibition.

In all the models subsequently developed, pIC_{50} values were used as the dependent variable. K_i is the inhibition constant for the drug; the concentration of competing ligand in a competition assay which would occupy 50% of the receptors if no ligand was present. The compounds from the dataset that are used for pharmacophore modeling are shown in **Table 1**.

TABLE 1: PYRIDINE-PYRIMIDINE ANALOGS (46 MOLECULES)¹⁴

S. no.	Structure	IC ₅₀ Value (nm)	pIC ₅₀ Value (nm)	Pharm Set	S. no.	Structure	IC ₅₀ Value (nm)	pIC ₅₀ Value (nm)	Pharm Set
1		1.7	8.7695		2		18	7.744	
3		17	7.769		4		570	6.244	
5		950	6.022		6		15200	4.818	Inactive
7		8200	8.200		8		2.8	8.552	
9		3.9	8.408		10		1.7	4.523	
11		30000	4.5228	Inactive	12		12	7.920	
13		18	7.442		14		1.1	8.9586	
15		1.75	8.7695		16		0.70	9.1549	Active
17		0.69	9.1611	Active	18		3.4	8.4685	

19		0.69	9.158	Active	20		1.3	8.886	Active
21		0.81	9.091		22		1250	5.903	
23		1.8	8.744		24		4.5	8.346	
25		18	7.745		26		34	7.468	
27		72	7.142		28		160	6.795	
29		200	6.698		30		1130	5.948	
31		600	6.221		32		30000	4.515	Inactive
33		2700	5.686		34		540	6.267	
35		170	6.769		36		173	7.301	

37		50	7.212	38		19	7.356
39		380	6.420	40		16500	4.782 Inactive
41		83	7.080	42		110	6.958
43		14	7.853	44		320	6.494
45		220	6.657	46		44	7.356

(C) Ligand Preparation: All molecules were built in Maestro 12.5, Schrodinger LLC, New York, NY, 2020, and prepared using LigPrep 2.5. LigPrep was used to convert the two-dimensional structure to a three-dimensional structure, generate stereoisomers, determine the most probable ionization state at user-defined pH of 7.4, neutralize the charged structure, add hydrogen, and generate the energy-minimized conformers using ConfGen (LigPrep version 2.5, Schrodinger) by applying optimized potentials for liquid simulations (OPLS3e) force field¹⁶.

Methodology: Pharmacophore modeling was carried out using Phase Schrodinger 20.0.3, LLC, New York, NY, 2020 implemented in Maestro 12.5.

Defining the Ligand Set for Model Development: The defining of the ligand set (the “pharm set”) that was to be used for model development was done by setting a threshold. The ligand set included some active ligands and

inactive ligands. The ligands marked as active in the Pharm Set column of the Ligands table were used to develop the model. The ‘Activity Thresholds’ option was clicked to set thresholds for active and inactive ligands. In the activity Thresholds dialog box, a threshold for the active ligands and inactive ligands was set. Ligands with activity greater than or equal to the active threshold were marked as active and included in the pharm set. Ligands with activity less than the inactive threshold were marked as inactive and included in the pharm set. Ligands whose activity lies between the thresholds were excluded from the pharm set^{15, 17, 18, 19}.

Creation of Pharmacophore Site: In this step, a set of chemical structure patterns was used to identify pharmacophore features in each ligand. Once a feature has been mapped to a specific location in conformation, it is referred to as a pharmacophore site. Phase Schrodinger20.0.3, LLC, New York, NY, 2020 provides a standard set of six pharmacophoric features, *i.e.*, a hydrogen

bond acceptor (A), a hydrogen bond donor(D), a hydrophobic group (H), and a negatively ionizable (N), positively ionizable (P), and aromatic ring (R) to define the chemical features of ligands^{15, 17, 18, 20}.

Generation of Common Pharmacophore Hypothesis:

Hypotheses were generated by systematic variation of the number of sites and the number of matching active compounds. Three to seven sites could be specified for the generation of the common pharmacophore hypothesis. However, an optimum number of sites were to be specified as each site represents 2-3 kcal/mol interaction with the receptor. Hence, a five-point common pharmacophore hypothesis was identified from all the conformations of the active ligands having an identical set of features with a very similar spatial arrangement. The pharmacophores that were common in all the active compounds were identified using a tree-based partitioning algorithm and studied further. Maximum tree depth specifies the number of binary partitioning steps used to sort the pharmacophore into similar groups. A tree depth of five was used to identify the common five variant pharmacophores. A minimum intersite distance of 2.0 °A was used. Minimum Intersite distance specifies the minimum distance allowed between two features. If the features in the ligand were closer than this distance, the hypothesis was rejected. The common pharmacophore hypothesis was considered, which indicated all five sites common to all molecules^{15, 17-19}.

Scoring Pharmacophore Hypothesis: The scoring procedure helps in ranking of the different hypotheses to yield the best alignment of the active ligands using an overall maximum root mean square deviation value of 1.2 °A with default options for distance tolerance. Thus, it helps in making a rational choice regarding which hypothesis is more appropriate for further investigation. The hypotheses generated were scored and ranked to find out the best possible hypothesis. The scoring for active and inactive was done using the default survival score weighting factors (vector score=1.0, reference ligand relative conformational energy = 0.0, and reference ligand activity = 0.0). There were several hypotheses of a given variant that looked very much alike and had very similar scores. In this situation, it was useful to cluster these hypotheses, using a suitable

clustering algorithm, and showing only a single representative from each cluster. Complete Clustering of similar hypotheses was done and the hypotheses were visualized by using 'Highest Average Similarity' mode from the view clusters dialog box^{15, 17, 18, 19}.

Building QSAR Models: The main purpose of developing the QSAR model was to predict the biological activities of new compounds whereby the generated model would be statistically robust, both internally and externally. The dataset was divided into a training set and a test set. 70% of molecules were taken in the training set and 30% in the test set. Atom-based 3D- QSAR models were generated for hypotheses. The QSAR model partitions the space occupied by the ligands into a cubic grid. Any structural component can occupy part of one or more cubes. A cube is occupied by an atom or a feature if its centroid is within the radius of the atom or feature. You can set the size of the cubes by changing the values in the Grid spacing text box. The allowed range is 0.5 °A to 2.0 °A. The default grid spacing of 1.00 °A was used. The regression was done by constructing a series of models with an increasing number of PLS factors. The accuracy of the models increases with an increasing number of PLS factors until over-fitting starts to occur. The maximum number of PLS factors is N/5, where N is the number of ligands in the training set.

Thus, the Maximum number of PLS factors used was 3 for pharmacophore built using the pyridine-pyrimidine class of compounds. The robustness of the developed pharmacophore hypotheses was internally validated by statistical parameters, including the squared correlation coefficient (R^2), q^2 (R^2 for test set), the standard deviation of regression, Pearson's correlation coefficient (Pearson's R), and variance ratio (F)^{15, 17, 18, 19}.

CONCLUSION: The present work aimed to develop pharmacophore models for pyridine-pyrimidine analogs which act as inhibitors of Merkinase. 10 models were generated and validated using atom-based QSAR. DDHRR-1 was selected as the best pharmacophore model based on the QSAR equation as well as the ability of pharmacophore to differentiate between active and inactive, based on site matches.

This model can be used for database screening to design and develop new inhibitors of Mer kinase in search of effective anticancer therapy.

Ethics Approval and Consent to Participate: Not applicable

Human and Animal Rights: No animals/ humans were used for studies.

Availability of Data and Materials: Not applicable

FUNDING STATEMENT: None

SUPPLEMENTARY MATERIAL: None

ACKNOWLEDGEMENT: The authors are thankful to the Pharmacy council of India and Schrodinger for providing software and The principal, S.N.J.B's S.S.D.J. College of Pharmacy, Neminagar, Chandwad, Nashik, Maharashtra, India, 423 101, for providing the necessary facilities to perform this research work.

CONFLICTS OF INTEREST: None

REFERENCES:

- Schmitz R, Freire VA, Yerbes R, Richter SV, Kahlert C, Loges S, Weitz J, Schneider M, Almodovar CR, Ulrich A and Schmidt T: TAM receptors Tyro3 and Mer as novel targets in colorectal cancer. *Oncotarget* 2016; 7: 56355-70.
- Chen J, Carey K and Godowski PJ: Identification of Gas6 as a ligand for Mer, a neural cell adhesion molecule related receptor tyrosine kinase implicated in cellular transformation. *Oncogene* 1997; 14(7): 2033-39.
- Caberoy NB, Zhou Y and Li W: Tubby and Tubby like protein 1 are new MerTK ligands for phagocytosis. *EMBO J* 2010; 29(23): 3898-3910.
- Caberoy NB, Alvarado G, Bigcas JL and Li W: Galectin-3 is a new MerTK-specific eat-me signal. *J. Cell. Physiol.* 2012; 227(2): 401-07.
- Linger RMA, Keating AK, Earp HS, Graham DK: TAM Receptor Tyrosine Kinase: Biologic Functions, signalling, and Potential Therapeutic Targeting in Human Cancer. In *advances in cancer Research*; Academic Press: New York, 2008; 100, 35-83.
- Graham DK, Salzberg DB, Kurtzberg J, Sather S, Matsushima GK, Keating AK, Liang X, Lovell MA, Williams SA, Dawson TL, Schell MJ, Anwar AA, Snodgrass HR and Earp HS: Ectopic expression of the proto-oncogene Mer In pediatric T-cell acute lymphoblastic leukemia. *Clin. Cancer. Res* 2006; 12(9): 2662-69.
- Linger RM, Cohen RA, Cummings CT, Sather S, Migdall-Wilson J, Middleton DH, Lu X, Baron AE, Franklin WA, Merrick DT, Jedlicka P, Deryckere D, Heasley LE and Graham DK: Mer or Axl receptor tyrosine kinase inhibition promotes apoptosis, blocks growth and enhances chemosensitivity of human non-small cell lung cancer. *Oncogene* 2013; 32: 3420-3431.
- Liu J, Zhang W, Stashko MA, DeRyckere D, Cummings CT, Hunter D, Yang C, Jayakody CN, Cheng N, Simpson C, Norris-Drouin J, Sather S, Kireev D, Janzen WP, Earp HS, Graham DK, Frey SV and Wang X: UNC1062, a new and potent Mer inhibitor. *Eur J Med Chem* 2013; 65: 83-93.
- Schlegel J, Sambade MJ, Sather S, Moschos SJ, Tan AC, Wingses A, Deryckere D, Carson CC, Trembath DG, Tentler JJ, Eckhardt SG, Kuan PF, Hamilton RL, Duncan LM, Miller CR, Nikolaishvili-Feinberg N, Midkiff BR, Liu J, Zhang W, Yang C, Wang X, Frey SV, Earp HS, Shields JM and Graham DK: MERTK receptor tyrosine kinase is a therapeutic target in melanoma. *J Clin Invest* 2013; 123(5): 2257-67.
- Tsou W, Nguyen K, Calabrese D, Garforth S, Antes A, Smimov S, Almo S, Birge R and Kotenko S: Receptor Tyrosine Kinases, TYRO3, AXL, and MER, Demonstrate Distinct Patterns and Complex Regulation of Ligand-induced Activation. *The Journal of Biology Chemistry* 2014; 289: 25750-763.
- Schmitz R, Freire VA, Yerbes R, Richter SV, Kahlert C, Loges S, Weitz J, Schneider M, Almodovar CR, Ulrich A and Schmidt T: TAM receptors Tyro3 and Mer as novel targets in colorectal cancer. *Oncotarget*. 2016; 7: 56355-370.
- Miles AM, Eunha K, Michael FC, Alec LP, Mark P, Rainer HK, Mikael P and Ralph W: Near-infrared imaging of Mer tyrosine kinase (MerTK) using MERi-SiR reveals tumor-associated macrophage uptake in metastatic disease. *Royal Society of Chemistry* 2012; 00: 1-3.
- Baladi T, Abet V and Sandrine P: State of the art of small molecules inhibition of the TAM family: the point of view of the chemist. *European Journal of Medicinal Chemistry* 2015; 1-39.
- Weihe Z, Dehin Z, Michael AS, Deborah DeRyckere D, Hunter DK, Michael JM, Christopher C, Minjung L, Jacqueline ND, Wendy MS, Susan S, Yingqiu Z, Gregory K, Mischa M, Wiliam PJ, HShelton E, Douglas KG, Stephen V and Xiaodong W: Pseudo-Cyclization through Intramolecular Hydrogen Bond Enables Discovery of pyridine Substituted pyrimidines as New Mer Kinase Inhibitors. *J of Medicinal Chemistry* 2013; 56: 9683-92.
- Small-Molecule drug Discovery Suite 2013: Phase, version 3.0, User Manual, Schrodinger, LLC, New York, NY, 2020.
- Small-Molecule Drug Discovery Suite 2013: Ligprep, version 2.5, User Manual, Schrodinger, LLC, New York, NY, 2020.
- Kulkarni VM and Bhansali SG: Pharmacophore generation, atom-based 3D-QSAR, docking, and virtual screening studies of p38- α mitogen-activated protein kinase inhibitors: Pyridopyridazin-6-ones (part 2). *Res Rep Med Chem* 2014; 1-21.
- Vyas VK, Ghate M and Goel A: Journal of Molecular Graphics and Modelling Pharmacophore modelling, virtual screening, docking and *in-silico* ADMET analysis of protein kinase B (PKB) inhibitors. *J Mol Graph Model* 2013; 42: 17-25.
- Zhang W, Xia S, Ye J, Tang Y, Li Z, Zhu W and Cheng J: Structural feature of GABAA receptor antagonists: Pharmacophore modeling and 3D-QSAR studies. *Med Chem Res* 2013; 22(12): 5961-72.
- Ugale VG, Patel HM and Surana SJ: Molecular modeling studies of quinoline derivatives as VEGFR-2 tyrosine

- kinase inhibitors using pharmacophore-based 3D-QSAR and docking approach. *Arab J Chem* 2013; 1-24.
21. Dixon SL, Smondyrev AM and Rao SN: PHASE: A novel Approach to Pharmacophore Modelling and 3D Database Searching 2006; 370-72.
 22. Dixon SL, Smondyrev AM, Knoll EH, Rao SN, Shaw DE and Friesner RA: PHASE: A new engine for pharmacophore perception, 3D QSAR model development, and 3D database screening: 1. Methodology and Preliminary Results. *J Comput Aided Mol Des* 2006; 20(10-11): 647-71.
 23. Chayan A, Andrew C, James EP and Alexander DM: Recent Advances in Ligand-Based Drug Design: Relevance and Utility of the Conformationally Sampled Pharmacophore Approach. *Current Computer-Aided Drug Design* 2011; 7: 10-22.
 24. Dror O, Schneidman DD, Inbar Y, Nussinov R and Wolfson HJ: Novel approach for efficient pharmacophore-based virtual screening: Method and applications. *J Chem Inf Model* 2009; 49(10): 2333-43.
 25. Gaurav A and Gautam V: Structure-based three-dimensional pharmacophores as an alternative to traditional methodologies. *J Receptor Ligand Channel Res* 2014; 7: 27-38.
 26. Xia J, Tilahun EL, Reid T, Zhang L and Wang XS: Benchmarking methods and data sets for ligand enrichment assessment in virtual screening. *Methods*, 2014, xxx xxx-xxx(article in press as: J. Xia et al., *Methods* (2014), <http://dx.doi.org/10.1016/i.ymeth.2014.11.015>, Accessed on April 12th, 2015).
 27. Kayla VM, Sarah RA and Kenneth JP: Targeting Tyro3, Axl and MerTK (TAM receptors): implications for macrophages in the tumor microenvironment. *Molecular Cancer* 2019; 18: 94.
 28. Shi C, Li X and Wang X: The proto-oncogene Mer tyrosine kinase is a novel therapeutic target in mantle cell lymphoma. *J Hematol Oncol* 2018; 11: 43.
 29. Rios DJ, Favata M, Lasky K, Feldman P, Lo Y, Yang G, Stevens C, Wen X, Sehra S, Katiyar K, Liu K, Wynn R, Harris JJ, Ye M, Spitz S, Wang X, He C, Li Y-L, Yao W, Covington M, Scherle P and Koblisch H: A Potent and Selective Dual Inhibitor of AXL and MERTK Possesses Both Immunomodulatory and Tumor-Targeted Activity. *Front. Oncol* 2020; 10: 598477.

How to cite this article:

Wagh S and Wagh V: Pharmacophore based modelling of pyridine-pyrimidine analogs as mer tyrosine kinases inhibitors in anticancer therapy. *Int J Pharm Sci & Res* 2021; 12(11): 5905-15. doi: 10.13040/IJPSR.0975-8232.12(11).5905-15.

All © 2021 are reserved by the International Journal of Pharmaceutical Sciences and Research. This Journal licensed under a Creative Commons Attribution-NonCommercial-ShareAlike 3.0 Unported License.

This article can be downloaded to **Android OS** based mobile. Scan QR Code using Code/Bar Scanner from your mobile. (Scanners are available on Google Playstore)